Electrocardiogram Signal Denoising by Hilbert Transform and Synchronous Detection

Mohammed Assam Ouali, Asma Tinouna, Mouna Ghanai, Kheireddine Chafaa

LASS Laboratory, Electronics Departement, Faculty of Technology
University of M'sila, Algeria
E-mails: mohamedassam.ouali@univ-msila.dz,
asma.tinouna@yahoo.com,
mouna.ghanai@mail.univ-batna.dz,
kheireddine.chafaa@mail.univ-batna.dz

Corresponding author

Received: July 30, 2019 **Accepted: May 06, 2020**

Published: December 31, 2020

Abstract: *An efficient method for Electrocardiogram (ECG) signal denoising based on synchronous detection and Hilbert transform techniques is presented. The goal of the method is to decompose a noisy ECG signal into two components classified according to their energy: (1) component with high energy representing the dominant component which is the clean ECG signal, and (2) component with low energy representing the sub-dominant component which is the contaminant noise. The investigated approach is validated through out some experimentations on MIT-BIH ECG database. Experimental results show that random noises can be effectively suppressed from ECG signals.*

Keywords: *ECG signals, ECG denoising, Hilbert transform, Synchronous detection.*

Introduction

Electrocardiogram (ECG) is a bioelectrical signal, which records the heart's electrical activity versus time [6, 16, 20]. It is an important diagnostic tool for assessing heart function. The ECG is a time varying signal which is neither periodic nor deterministically chaotic (the interbeat intervals seems to contain a random component). Each phase of cardiac electrical activity produces a specific wave or a complex one. The basic ECG waves are labelled alphabetically as P wave, QRS complex, ST segment and T wave [1]. During ECG measurement, noise (anything other than muscular activity of heart) is superimposed on it, due to AC interference, loose electrode connection, malfunctioning of machine, patient movement like respiration etc., all of them collectively called artefacts. Hence, extraction of clean ECG signal from noisy measurements is needed and this is one of the big problems in biomedical signal processing. Latest contributions in this subject are reported in [7–9, 15, 18–21, 23, 25].

In the last few years, many researchers have proposed methods and approaches for ECG signal denoising. Wavelet transform is generally employed for ECG denoising due to its ability to characterize time-frequency domain information of a time domain signal. Yadav et al. [25] have proposed a novel non-local wavelet transform (NLWT) method for ECG signal denoising by exploiting the local and non-local redundancy present in the signal. Smital et al. [18] developed a method using dyadic stationary wavelet transform (SWT) in the Wiener filter for the estimation of a noise-free signal. The number of decomposition levels and the impulse characteristics are the two most important factors considered in SWT.

A method based on sparse derivatives (SD) was presented by Ning et al. [15] where the artefacts are reduced by modeling the clean ECG signal as a sum of two signals whose second and third-order derivatives are sparse respectively. Tracey and Miller [21] suggested using a non-local means (NLM) approach to denoise ECG signals. This method can provide efficient denoising while minimizing signal distortion. Lahmiri [9] in its work presented a comparative study of ECG signal denoising by wavelet thresholding in empirical mode decomposition - discrete wavelet transform (EMD-DWT) and variational mode decomposition - discrete wavelet transform (VMD-DWT) domains. According to this work, the VMD can outperform the EMD in denoising the ECG signal. In addition, the NLM technique was adopted as a reference model, which was recently found to be effective in denoising ECG signals.

Adaptive filtering method has been recently proposed for ECG signal denoising. The method presented in [7] is based on two algorithms. The first one is a DWT for denoising, and the second is an adaptive dual threshold filter (ADTF). Wang et al. [23] presented a method based on the adaptive Fourier decomposition (AFD). This method is based on the assumption that the energy of the pure ECG signal is higher than that of the noise. Kumar et al. [8] proposed a method using EMD with NLM for the cancellation of noise. In this method, the edges of the ECG signal are successfully preserved. Tinouna et al. [20] developed a simple and efficient method to remove white Gaussian noises and physiological noises from ECG signals based on simple tools usually used in digital signal processing like moving average filter, median filter, baseline drift removal and peak detection.

In this paper we propose to use the Hilbert transform and the multi-component representation of analytical signal with the synchronous detection method for ECG signal denoising. This method extracts the mono-components of a signal by using its analytic form where the first component corresponds to the highest instantaneous amplitude [3, 4]. The component with the highest instantaneous amplitude is referred as the dominant component of the signal. The high oscillating part with lowest instantaneous amplitude is referred as the sub-dominant component of the signal (noise), so the first step of the method is to estimate the instantaneous frequency of the largest energy component and then use the synchronous detection approach to extract the amplitude details about this component.

The impact of the proposed filtering method on the distortion of diagnostic features of the ECG was investigated using an ECG diagnostic distortion measure called the "Multi-Scale Entropy Based Weighted Distortion Measure" or MSEWPRD. The closer this criteria is to zero, the better the morphological characteristics of the ECG signal are preserved. Experimental results reveal that the proposed algorithm have low MSEPWRD for all noise types at low input SNRs, which can much better conserve the morphology and diagnostic information of ECG signals. Therefore, the morphology and diagnostic information of ECG signals were much better conserved, compared to the results presented in [5].

Preliminaries

The Hilbert transform and the analytical signal representation

The analytical signal $H(t)$ of a real signal $X(t)$ is a complex signal as given by [17]:

$$H(t) = X(t) + X_H(t) = A(t)\exp^{\phi(t)}. \tag{1}$$

This analytical representation enables computation of the instantaneous phase ϕ, the instantaneous frequency (IF), $\omega(t) = d\phi(t)/dt$, and the instantaneous amplitude (IA) $A(t)$ as follows:

$$A(t) = \sqrt{X^2(t) + X_H^2(t)}, \tag{2}$$

$$\phi(t) = \tan^{-1}\left(\frac{X_H(t)}{X(t)}\right). \tag{3}$$

The IF is the derivative of $\phi(t)$ expressed as:

$$\omega(t) = \frac{d}{dt}\phi(t) = \frac{X(t)\dot{X}_H(t) - \dot{X}(t)X_H(t)}{X^2(t) - X_H^2(t)}, \tag{4}$$

where $X_H(t)$ is the Hilbert transform of $X(t)$ given as:

$$H[X(t)] = \tilde{X}(t) = \pi^{-1}\int_{-\infty}^{+\infty}\frac{X(\tau)}{t-\tau}d\tau. \tag{5}$$

The Hilbert transform acts as a phase shifter where the signal's amplitude is unchanged and phase is shifted by $\pi/2$. In other words, the analytic signal rotates in the z-plane with a rate of rotation determined by $\omega(t)$. The IA and rate of rotation do not change for monoharmonic signals, whereas more complicated multi-component signals have time-varying spectral dynamics [14, 22].

One can express a multi-component signal (assume that the orignal signal $X(t)$ is a multi-component signal) using the composition of separate mono-component part as:

$$X(t) = \sum_k X_k(t) = \sum_k a_k(t)\cos\left(\int \omega_k(t)dt + \theta_k\right), \tag{6}$$

where $a_k(t)$ is the IA, $\omega_k(t)$ is the IF of the k component and θ_k is the phase offset. Here k indicates the different components having different oscillatory frequencies and amplitudes.

ECG signals

In this investigation we compare our method with various benchmark methods recently published and presented in [24]. For this purpose, we use synthetic ECGs generated by an ECG dynamical model [12] and real ECGs signals taken from MIT-BIH database [13].

ECG dynamical model

McSharry [12] proposed a synthetic ECG dynamical generator constituted of three-dimensional state equations (Eq. (7)), which can generate a trajectory in the Cartesian coordinates:

$$\begin{cases} \dot{x} = \alpha x - \omega y, \\ \dot{y} = \alpha y + \omega x, \\ \dot{z} = -\sum_i a_i \Delta\theta_i \exp\left(\frac{-\Delta\theta_i^2}{2b_i^2}\right) + (z - z_0), \end{cases} \tag{7}$$

where $\alpha = 1 - \sqrt{x^2 + y^2}$, $\Delta\theta_i = (\theta - \theta_i)mod(2\pi)$, $\theta = atan2(x, y)$ ($atan2$ is the four quadrant arctangent of the real parts of the elements of x and y), with $-\pi < atang2(x, y) < \pi$, and ω is the angular velocity of the trajectory as it moves around the limit cycle.

This model has many adjustable parameters, which makes it adaptable to many normal and abnormal ECG signals, such as a_i, b_i, θ_i and z_0, which corresponds to amplitude, width, center parameters of the Gaussians and the baseline drift, respectively.

Real ECG signals
The real ECG data are taken from the MIT-BIH database [13]. The MIT-BIH arrhythmia database contains 48 excerpts of 30 min each of two-channel ambulatory ECG recordings, obtained from 47 subjects studied by the BIH Arrhythmia Laboratory between 1975 and 1979. Twenty-three recordings were chosen at random from a set of 4000 ambulatory ECG recordings of 24 h each collected from a mixed population of inpatients (about 60%) and outpatients (about 40%) at Boston's Beth Israel Hospital. The remaining 25 recordings were selected from the same set to include the less common but clinically significant arrhythmias that would not be well represented in a small random sample. The recordings were digitized at 360 samples per second per channel with 11-bit resolution over a range of 10 mV. Two or more cardiologists annotated each record independently. Disagreements were resolved to obtain the computer-readable reference annotations for each beat (approximately 110,000 annotations in total) included with the database.

Evaluation criteria

For evaluation purposes, signal to-error-ratio (SER) and the mean squared error (MSE) criteria will be used. These evaluators are defined as follows:

$$SER = 10 \times log\left(\frac{\sum_i |x_c(i)|^2}{\sum_i |x_c(i) - \hat{x}(i)|^2}\right), \tag{8}$$

$$MSE = \frac{1}{N}\sum_i (x_c(i) - \hat{x}(i))^2, \tag{9}$$

where, x_c is the clean ECG, $\hat{x}$ is the denoised ECG signal, and N is the number of samples.

For the evaluation in terms of preserving the diagnostic features of the ECG signal we have used an ECG diagnostic distortion measure called the Multi-Scale Entropy based Weighted Distortion Measure [5, 11]. We used a similar method as that utilized in [5] to calculate this measure. A Weighted Percentage Root Square Difference (WPRD) is used for the metric, which is generated by comparing the original sub-band wavelet coefficient with the filtered signals. This uses weights that are the same as the corresponding sub-band's multi-scale entropies. Using this measure, it is possible to achieve an accurate representation of the distortion of the filtered signal at all sub-bands [5, 11]. It was necessary to decompose both signals using wavelet filters up to L level in order to calculate this metric. Both the sampling frequency and the nature of the signal dictate the number of levels. An accurate ECG trace will include a sharp QRS complex segment and the slow P and T waves, therefore, an effective decomposition of an ECG should display an effective representation of the details coefficients of the QRS complexes and the approximation coefficients of the P and T waves. As such, Daubechies 9/7 bi-orthogonal wavelet filter [2] was used for decomposition purposes. This led us to choose $L = 4$ for sampling frequency of 128 Hz [10].

The Multiscale entropy-based WPRD measure is defined as:

$$MSEWPRD = w_{A_L} \times \left(\sqrt{\frac{\sum_{k=1}^{N_{A_L}} [A_L(k) - \tilde{A}_L(k)]^2}{\sum_{k=1}^{N_{A_L}} [A_L(k)]^2}} \times 100 \right) + \sum_{j=1}^{L} w_{D_j} \times \left(\sqrt{\frac{\sum_{k=1}^{N_{D_j}} [D_j(k) - \tilde{D}_j(k)]^2}{\sum_{k=1}^{N_{D_j}} [D_j(k)]^2}} \times 100 \right), \quad (10)$$

where w_{A_L} denotes the weight for the L^{th} approximation band; w_{D_j} denotes the weight for the j^{th} level details subband; A_L and $\tilde{A}_L$ denote the L^{th} approximation band coefficients of the original and the denoised signals, respectively; and D_j and $\tilde{D}_j$ denote the j^{th} details band coefficients of the original and the denoised signals, respectively. w_{A_L} and w_{D_j} are the weights.

ECG denoising method

The proposed method is based on the assumption that the noisy ECG signal $x(t)$ is a sum of quasi-harmonics components (Eq. (6)), which are the dominant component (clean ECG signal) and the sub-dominant component (noise). The procedure of the method is described as follows:

- **Step 1.** Estimate IF of the largest component. In this case, the signal can be modelled as a weighted sum of mono-component signals, each with its own IF [22], and amplitude function:

  $$x(t) = a_1(t)\exp^{i\int_0^t \omega_1(t)dt} + a_2(t)\exp^{i\int_0^t \omega_2(t)dt}. \quad (11)$$

  Assuming that $a_1(t)$ is larger than $a_2(t)$, the envelope $a(t)$ and the IF $\omega(t)$ of the double-component signal $x(t)$ are given as follows:

  $$a(t) = \left[a_1^2 + a_2^2 + 2a_1a_2\cos\left(\int(\omega_2 - \omega_1)dt\right)\right]^{1/2}, \quad (12)$$

  $$\omega(t) = \omega_1 + \frac{(\omega_2 - \omega_1)[a_2^2 + 2a_1a_2\cos(\int(\omega_2 - \omega_1)dt)]}{a^2(t)}. \quad (13)$$

  The envelope signal $a(t)$ consists of two different parts:

  1: A rapidly varying part;

  2: A slow varying part including the sum of the amplitude components squared.

  The IF $\omega(t)$ contains also two parts:

  1: A gradual altering frequency of the first component ω_1;

  2: An asymmetrical oscillating component which changes rapidly based on the frequency.

The integration of the oscillating part with the integration limits on the full period of the difference frequency $[0 \quad T = 2\pi/(\omega_2 - \omega_1)]$ will become zeros as follows:

$$\int_0^T \frac{(\omega_2 - \omega_1)[a_2^2 + 2a_1 a_2 \cos(\int(\omega_2 - \omega_1)dt)]}{a^2(t)} = 0. \tag{14}$$

Therefore, the second component which is the rapidly varying asymmetrical oscillating part can be removed with low-pass filtering, where the cut-off frequency is equal to the heartbeat frequency, and the remaining frequency ω_1 is the largest harmonic frequency.

- **Step 2.** Obtain the corresponding envelope of the largest component, for this purpose we use the synchronous detection method. This technique extracts the amplitude details about the vibration components by multiplying the initial signal $x(t)$ by two reference signals exactly 90° out of phase with one another. First, the reference signals is defined as:

$$r_1(t) = \cos\left(\int \omega_l(t)\right), \tag{15}$$

$$r_2(t) = -\sin\left(\int \omega_l(t)\right). \tag{16}$$

Then, we multiply $x(t)$ by $r_1(t)$ and $r_2(t)$ to obtain the in-phase signal $x_1(t)$ and the quadrature signal $x_2(t)$, respectively, as follows:

$$x_1(t) = \frac{1}{2}a_{k=l}(t)\left[\cos(\theta_{k=l}) + \cos\left(\int(\omega_{k=l} + \omega_l)dt + \theta_{k=l}\right)\right], \tag{17}$$

$$x_2(t) = \frac{1}{2}a_{k=l}(t)\left[\sin(\theta_{k=l}) + \sin\left(\int(\omega_{k=l} + \omega_l)dt + \theta_{k=l}\right)\right]. \tag{18}$$

Each of the obtained signals in Eqs. (17) and (18) consists of two different functions. The first one is the slow varying function and the other is a fast-oscillating part. In such case, it is possible to remove the oscillating part again by using low-pass filter (with the cut-off frequency is equal to the heartbeat one). Thus, only the slow varing part will be retained, and the IA and the phase offset of the l^{th} component can be respectively given by:

$$a_l(t) = 2\sqrt{(\tilde{x}_1(t))^2 + (\tilde{x}_2(t))^2}, \tag{19}$$

$$\theta_l = \arctan\frac{\tilde{x}_2(t)}{\tilde{x}_2(t)}, \tag{20}$$

where, $\tilde{x}_1$ and $\tilde{x}_2$ are the filtered result of $x_1(t)$ and $x_2(t)$ respectively, which are expressed as:

$$\tilde{x}_1(t) = \frac{1}{2}a_l(t)\cos(\theta_l), \tag{21}$$

$$\tilde{x}_2(t) = \frac{1}{2}a_l(t)\sin(\theta_l). \tag{22}$$

- **Step 3.** Subtract the largest component from the original signal $x(t)$, then, the second-largest component can be obtained by repeating the above steps. The number of iterations necessary to provide a good approximation depends on how rapidly the initial signal changes.

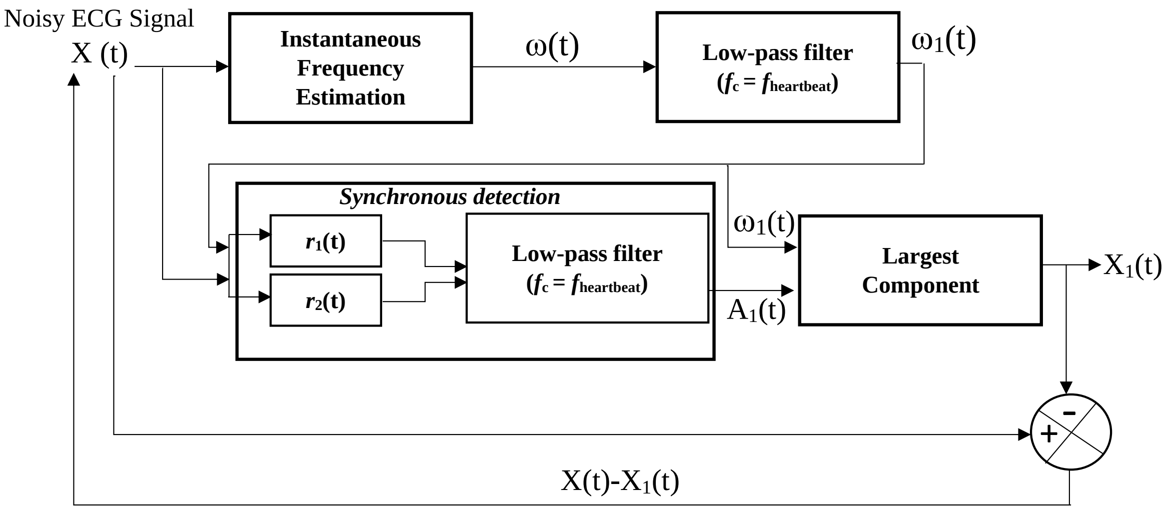

Fig. 1 Block diagram of the proposed method

The clean ECG signal can be reconstructed by a simple subtraction of the last component with a high oscillation from the initial signal. The block diagram of the investigated method is given by Fig. 1.

Results and discussions

In this section, simulation and experimental tests on both synthetic and real ECG signals are carried out to evaluate the performance of the investigated method.

Synthetic ECG signal denoising results

A synthetic ECG signal has been generated with the dynamical model discussed previously (see Eq. (7)). To synthesize a noisy ECG signal, Gaussian white noise is added to the generated ECG signal with $SNR_{input} = 5$ dB. The synthetic noisy ECG signal is then denoised by the investigated method. The denoising result is shown in Fig. 2, where it can be seen that the proposed approach is able to give a very good denoising result. In Fig. 3 we present the corresponding error (errors before and after denoising), where we note clearly that the error after denoising is smaller than the error before denoising, which confirms the efficiency of the proposed procedure for ECG denoising.

To evaluate quantitatively the denoising quality of the proposed method, *SER* (Eq. (8)) and *MSE* (Eq. (9)) are used as performance indices for denoising. *SER* defines the signal energy with respect to the energy of the error. *MSE* defines the energy of the error signal in the denoising process. Performance indices calculated under different levels of noise intensity (5 dB, 10 dB, 15 dB, and 20 dB) are listed in Table 1 in which we compared the results obtained by our method and those obtained by the methods presented in [24], namely Wavelet based method, EMD Partial Reconstruction method and CEEMDAN Plus Wavelet Threshold method.

From the Table 1 we can clearly see that the proposed method has the highest *SER* and lowest *MSE* under all noise intensities levels compared to the methods considered in [24]. These results demonstrates the superiority of the suggested method over other methods.

Real ECG signal denoising results

For real ECGs, records 100.dat and 103.dat are chosen from MIT-BIH arrhythmia database.

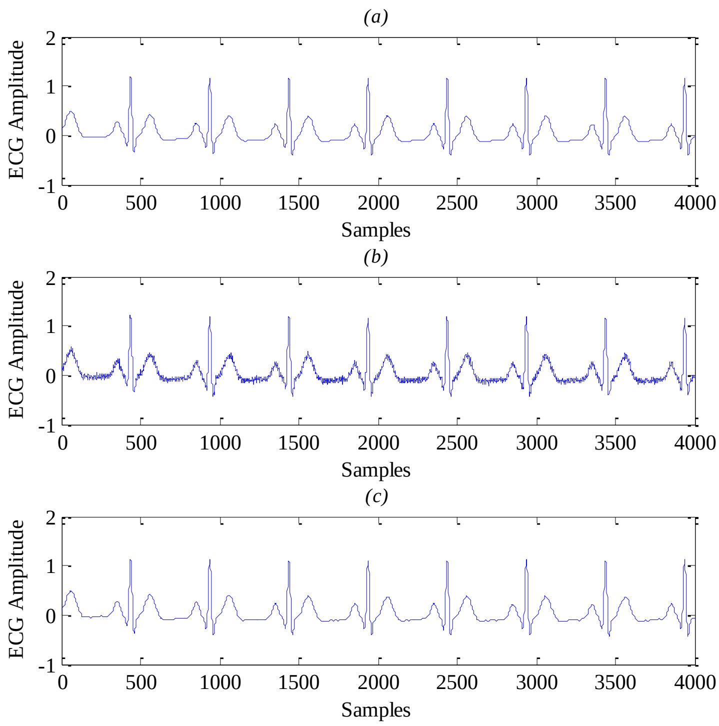

Fig. 2 Synthetic ECG denoising result:
a) the clean ECG signal; b) the corrupted ECG signal with $SNR_{input} = 5$ dB;
c) the denoised ECG signal.

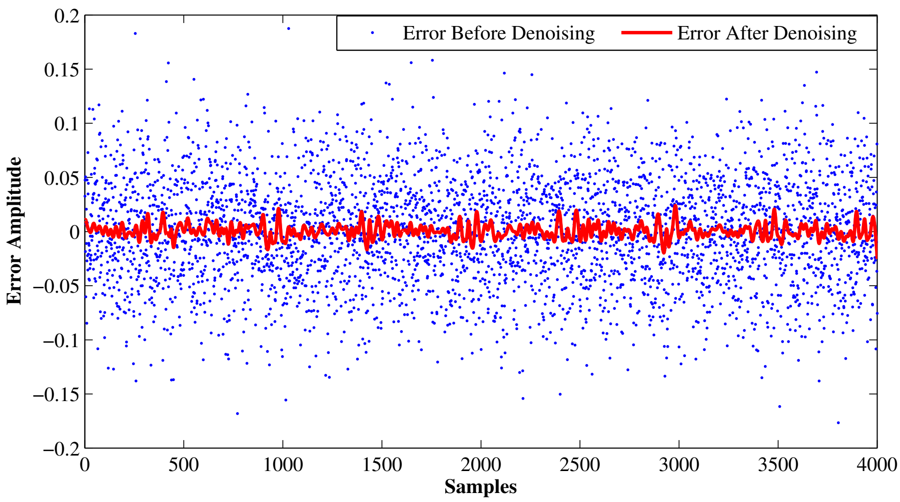

Fig. 3 Error before and after denoising

These signals are considered as clean, so we add to them white Gaussian noises with $SNR_{input} = 5$ dB in order to obtain corrupted ECGs. Visual inspections of Figs. 4 and 5 show the efficiency of the proposed technique.

Performance indices under different corrupting noise intensities are listed in Tables 2 and 3.

Once again, the Tables 2 and 3 clearly show that the proposed method has the highest *SER* and lowest *MSE* compared to the methods presented in [24], which demonstrates again the

Table 1. Performance indices under different noise intensities (Synthetic ECG)

Noise intensity	Index	Wavelet based	EMD partial reconstruction	CEEMDAN plus wavelet threshold	Proposed method
5 dB	*SER*	0.8751	6.8711	18.3150	18.590
	MSE	0.0452	0.0218	0.0016	0.00121
10 dB	*SER*	0.5978	5.9251	17.0436	17.7853
	MSE	0.0466	0.0271	0.0021	0.00187
15 dB	*SER*	0.4232	4.8161	12.5823	14.324
	MSE	0.0492	0.0295	0.0056	0.00321
20 dB	*SER*	0.2435	3.9363	10.4129	12.214
	MSE	0.0709	0.0638	0.0097	0.00698

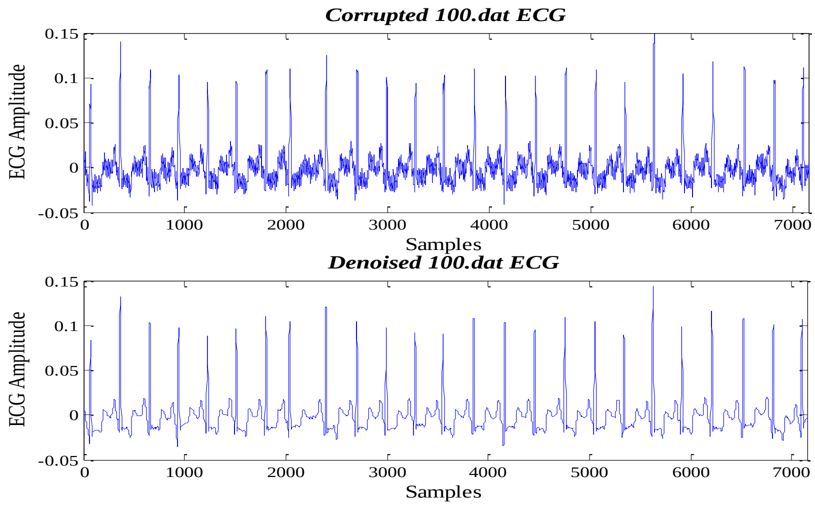

Fig. 4 Real ECG 100.dat denoising result

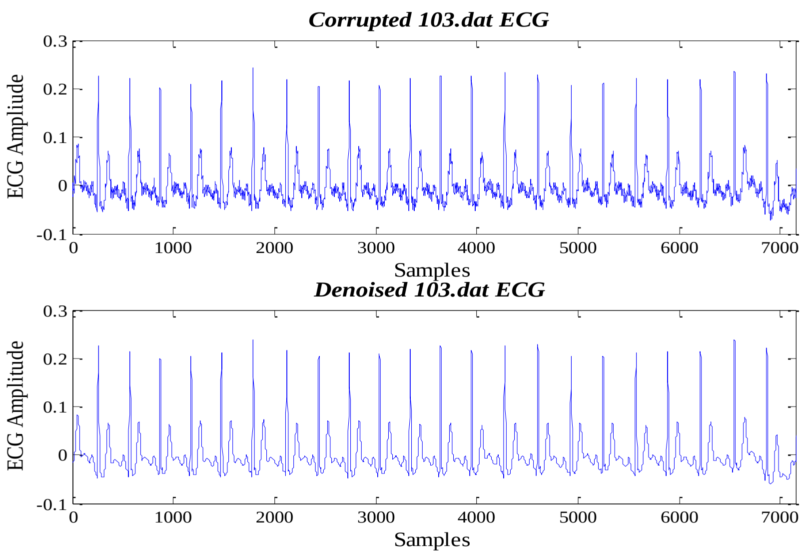

Fig. 5 Real ECG 103.dat denoising result

superiority of our method.

Further, we evaluate our method in terms of preserving the diagnostic features of the ECG signal. The ECG diagnostic distortion measure called Multi-Scale Entropy Based Weighted Distortion Measure (see Eq. (10)) is used. The closer this criteria is to zero, the better the morphological features are preserved. The MSEWPRD index is computed under different SNR_{input} levels and is listed in Table 4, which 4 confirms the efficiency of the proposed method in terms of preserving the diagnostic information and ECG morphology.

Table 2. Performance indices under different noise intensities (real ECG signal 100.dat)

Noise intensity	**Index**	**Wavelet based**	**EMD partial reconstruction**	**CEEMDAN plus wavelet threshold**	**Proposed method**
5 dB	*SER*	14.9580	17.9656	26.6223	27.0052
	MSE	0.0213	0.0096	0.0010	0.0008
10 dB	*SER*	12.8418	16.1767	24.8403	24.9845
	MSE	0.0235	0.0105	0.0016	0.0012
15 dB	*SER*	11.3410	14.8742	21.6968	22.1548
	MSE	0.0380	0.0124	0.0041	0.0038
20 dB	*SER*	10.3478	13.7996	17.8879	18.452
	MSE	0.0438	0.0198	0.01754	0.0069

Table 3. Performance indices under different noise intensities (real ECG signal 103.dat)

Noise intensity	**Index**	**Wavelet based**	**EMD partial reconstruction**	**CEEMDAN plus wavelet threshold**	**Proposed method**
5 dB	*SER*	14.7072	16.2526	27.8397	28.1875
	MSE	0.0210	0.0113	0.0006	0.0004
10 dB	*SER*	13.1222	15.6894	25.3689	25.9325
	MSE	0.0210	0.0129	0.0129	0.0009
15 dB	*SER*	11.7577	13.9286	20.4182	21.1587
	MSE	0.0316	0.0154	0.0035	0.0029
20 dB	*SER*	10.6856	11.9397	16.1626	17.452
	MSE	0.0405	0.0217	0.0095	0.0081

Table 4. Performance indices (MSEWPRD) under different SNR_{input} levels

ECG signal	**Index**	$SNR_{input} =$ **0 dB**	$SNR_{input} =$ **-1 dB**	$SNR_{input} =$ **-3 dB**	$SNR_{input} =$ **-5 dB**
Synthetic ECG	MSEWPRD	0.606	0.690	0.758	0.874
100.dat	MSEWPRD	0.4587	0.530	0.613	0.687
103.dat	MSEWPRD	0.4325	0.4521	0.609	0.668

Finally, in what follows, the proposed method was further tested against a model-based method described in [5], which detailed an ECG signal denoising method that utilized a marginalized particle extended Kalman filter. This used an automatic particle weighting strategy. The proposed method was compared to this method in terms of the MSEWPRD criterion. The results of the comparison between our method and the methods presented in [5], using the MSEWPDM with various SNR_{input} levels, are shown in Table 5. These results were generated by determining the MSEWPDMs of 200 filtered ECG segments that were selected from the MIT-BIH database. However, the chosen segments used in our algorithm can be not the same as those segments used in [5].

Table 5. Performance comparison between MP-EKF, EKS, EKF and the proposed method in the presence of white Gaussian noise from MSEPWRD viewpoint

Noise type	Method	MSEPWRD ($mean \mp SD$) (mv)			
		$SNR_{input} =$ **0 dB**	$SNR_{input} =$ **-1 dB**	$SNR_{input} =$ **-3 dB**	$SNR_{input} =$ **-5 dB**
White Gaussian noise	MP-EKF	1.284 ∓ 0.225	1.329 ∓ 0.224	1.434 ∓ 0.231	1.552 ∓ 0.242
	EKS	1.358 ∓ 0.180	1.458 ∓ 0.196	1.678 ∓ 0.237	1.9239 ∓ 0.288
	EKF	1.677 ∓ 0.183	1.824 ∓ 0.200	2.158 ∓ 0.242	2.552 ∓ 0.297
	Proposed method	$\mathbf{0.5158 \mp 0.065}$	$\mathbf{0.587 \mp 0.105}$	$\mathbf{0.674 \mp 0.051}$	$\mathbf{0.764 \mp 0.075}$

These results show that the MP-EKF and EKF/EKS had higher MSEWPDMs for the white Gaussian noise and at all of the SNR_{input} levels compared to the proposed method, indicating that the proposed method is more effective than the MP-EKF and EKF/EKS at preserving the diagnostic information and morphology of the ECG signals.

Conclusion

In this paper, Hilbert transform and synchronous detection was applied for ECG signal enhancement. The noisy ECG signal was decomposed in sub-components: the highest energy component representing the dominant component (ECG signal) and the lowest energy component representing the sub-dominant component (noise). Finally we extract the denoised ECG signal by a simple subtraction of the sub-dominant component from the noisy ECG signal. Simulation results showed that this technique is computationally efficient and have better performances under different power conditions of noise without affecting the morphology of the ECG signal.

References

1. Abedin Z., R. Conner (2008). ECG Interpretation: The Self-assessment Approach, John Wiley & Sons.
2. Antonini M. (1992). Image Coding Using Wavelet Transform, IEEE Transactions on Image Processing, 1(2), 205-220.
3. Feldman M. (2006). Time-varying Vibration Decomposition and Analysis Based on the Hilbert Transform, Journal of Sound and Vibration, 295(3-5), 518-530.
4. Feldman M. (2011). Hilbert Transform Applications in Mechanical Vibration, John Wiley & Sons.
5. Hesar H., M. Maryam (2016). ECG Denoising Using Marginalized Particle Extended Kalman Filter with an Automatic Particle Weighting Strategy, IEEE Journal of Biomedical and Health Informatics, 21(3), 635-466.
6. Jekova I., V. Tsibulko, I. Iliev (2014). ECG Database Applicable for Development and Testing of Pace Detection Algorithms, International Journal Bioautomation, 18(4), 377-388.

7. Jenkal W., R. Latif, A. Toumanari, A. Dliou, O. El Bacarri, F. M. Maoulainine (2016). An Efficient Algorithm of ECG Signal Denoising Using the Adaptive Dual Threshold Filter and the Discrete Wavelet Transform, Biocybernetics and Biomedical Engineering, 36(3), 499-508.
8. Kumar S., D. Panigrahy, P. K. Sahu (2018). Denoising of Electrocardiogram (ECG) Signal by Using Empirical Mode Decomposition (EMD) with Non-local Mean (NLM) Technique, Biocybernetics and Biomedical Engineering, 38(2), 297-312.
9. Lahmiri S. (2014). Comparative Study of ECG Signal Denoising by Wavelet Thresholding in Empirical and Variational Mode Decomposition Domains, Healthcare Technology Letters, 1(3), 104-109.
10. Manikandan M. S., D. Samarendra (2007). Wavelet Energy Based Diagnostic Distortion Measure for ECG, Biomedical Signal Processing and Control, 2(2), 80-96.
11. Manikandan M. S., D. Samarendra (2008). Multiscale Entropy-based Weighted Distortion Measure for ECG Coding, IEEE Signal Processing Letters, 15, 829-832.
12. McSharry P. E. (2003). A Dynamical Model for Generating Synthetic Electrocardiogram Signals, IEEE Transactions on Biomedical Engineering, 50(3), 289-294.
13. MIT-BIH Database, available at: http://www.physionet.org/physiobank/database/mitdb/.
14. Mutlu A. Y. (2018). Detection of Epileptic Dysfunctions in EEG Signals Using Hilbert Vibration Decomposition, Biomedical Signal Processing and Control, 40, 33-40.
15. Ning X., I. W. Selesnick (2013). ECG Enhancement and QRS Detection Based on Sparse Derivatives, Biomedical Signal Processing and Control, 8(6), 713-723.
16. Ouali M. A., M. Ghanai, K. Chafaa (2018). Upper Envelope Detection of ECG Signals for Baseline Wander Correction: A Pilot Study, Turkish Journal of Electrical Engineering & Computer Sciences, 26(2), 803-816.
17. Saxena N., K. S. Kamalesh (2017). Pansharpening Approach Using Hilbert Vibration Decomposition, IET Image Processing, 11(12), 1152-1162.
18. Smital L., M. Vitek, J. Kozumplik (2013). Adaptive Wavelet Wiener Filtering of ECG Signals, IEEE Transaction on Biomedical Engineering, 60(2), 437-445.
19. Tikkanen P. E. (1999). Nonlinear Wavelet and Wavelet Packet Denoising of Electrocardiogram Signal, Biological Cybernetics, 80(4), 259-267.
20. Tinouna A., M. Ghanai, M. A. Ouali, K. Chafaa (2019). Efficient Filtering Framework for Electrocardiogram Denoising, International Journal Bioautomation, 23(4), 403-420.
21. Tracey B. H., E. L. Miller (2012). Nonlocal Means Denoising of ECG Signals, IEEE Transactions on Biomedical Engineering, 59(9), 2383-2386.
22. Vakman D. (1998). Signals, Oscillations, and Waves, Artech House, Boston, London.
23. Wang Z., F. Wan, C. M. Wong, L. Zhang (2016). Adaptive Fourier Decomposition Based ECG Denoising, Computers in Biology and Medicine, 77, 195-201.
24. Xu Y., M. Luo, T. Li, G. Song (2017). ECG Signal De-noising and Baseline Wander Correction Based on CEEMDAN and Wavelet Threshold, Sensors (Basel), 17(12), 2754, doi: 10.3390/s17122754.
25. Yadav S. K., R. Sinha, P. K. Bora (2015). Electrocardiogram Signal Denoising Using Non-local Wavelet Transform Domain Filtering, IET Signal Processing, 9(1), 88-96.

Assoc. Prof. Mohammed Assam Ouali, Ph.D.
E-mail: mohamedassam.ouali@univ-msila.dz

Mohammed Assam Ouali received an Engineer degree in Electronics from M'sila University, a Master degree from M'sila University, Algeria and a Ph.D. degree in 2018 from Batna University, Algeria. Currently, he is an Associate Professor with the Department of Electronics at M'sila University. His research interests include biomedical engineering, dynamical modeling and digital signal processing.

Asma Tinouna, M.Sc.
E-mail: a.tinouna@univ-batna2.dz

Asma Tinouna received a Licence degree in Medical Instrumentation in 2008, and a Master degree in Biomedical Electronics from Batna University, Algeria, in 2010. Her research interests are in the field of biomedical signal processing.

Assoc. Prof. Mouna Ghanai, Ph.D.
E-mail: m.ghanai@univ-batna2.dz

Mouna Ghanai received an Engineer degree in Electronics from Batna 2 University in 1999 and the Master degree from Setif University, Algeria in 2006, and a Ph.D. degree in 2013 from Batna 2 University, Algeria. Currently she is an Associate Professor with the Department of Electronics, Batna 2 University. Her research interests include modelling and identification of nonlinear systems, automatic control and biomedical signal processing.

Prof. Kheireddine Chafaa, Ph.D.
E-mail: k.chafaa@univ-batna2.dz

Kheireddine Chafaa received an Engineer, a Master and a Ph.D. degrees in Electronics from Batna 2 University, Algeria in 1994, 1999 and 2006, respectively. Currently, he is a Professor with the Department of Electronics, Batna 2 University. His research interests include modelling and identification of nonlinear systems, nonlinear and adaptive control, soft computing and biomedical signal processing.